Analysis of the failure of a PPS polymer cycling support:

Marsh, Joseph; Turner, Richard; Wang, Minshi; Jenkins, Michael

DOI:
10.1016/j.engfailanal.2018.07.025

Document Version
Peer reviewed version

Citation for published version (Harvard):
Marsh, J, Turner, R, Wang, M & Jenkins, M 2018, 'Analysis of the failure of a PPS polymer cycling support: Microscopy and Finite Element studies', *Engineering Failure Analysis*, vol. 93, pp. 300-308. https://doi.org/10.1016/j.engfailanal.2018.07.025

To be submitted to: *Journal of Engineering Failure Analysis*

Analysis of the failure of a PPS polymer cycling support: Microscopy and Finite Element studies

J. Marsh, R.P. Turner*, M. Wang and M.J. Jenkins

School of Metallurgy & Materials, University of Birmingham, Edgbaston, Birmingham, United Kingdom B15 2TT

*email: r.p.turner@bham.ac.uk

Abstract

A PPS polymer injection moulded arm-support for cyclists has been developed to allow cyclists to position their arms parallel with the frame of the bicycle for aerodynamic improvement. The component is therefore subjected to both vertically applied force and laterally applied force. The vertical force comes from the weight of the cyclist transferring down through the shoulder to the elbow and forearm, which rest on the component, and the lateral force arising when the cyclist's arms try to push outwards for either power or stability. A component of this design suffered a sudden-onset fracture failure in-service. It was therefore of interest to understand why the component failed in this manner. The component was analysed by using electron microscopy methods at the fracture surface, performing a thermal testing analysis and mechanical data study of the reinforced PPS material to understand the material behaviour and lastly by using finite element (FE) analysis tools to predict the in-service mechanical fields of stress and strain. The resulting analyses highlighted that the failure was potentially caused by an abnormally high level loading, coupled with the potential for a manufacturing process induced void or defect which then acted as a nucleation site for a crack to propagate in the presence of a stress distribution.

1. Introduction

PPS, or polyphenylene sulfide, is a partially crystalline, high temperature performance polymer. PPS is polymerised by step growth polymerisation of para-dichlorobenzene (p-dcB) and sodium sulphide (Na_2S) (or sodium hydro sulphide (NaSH)): Na-S-Na + Cl-(C_6H_4)-Cl → -[C_6H_4S]- + 2 NaCl. The reaction is carried out in a polar solvent at elevated temperature and pressure [1].

Pure PPS is brittle by nature and as result it is not commonly used without being altered. To improve this brittle fracture, two methods can be implemented: 1) To modify the PPS chemical structure, introducing polar groups in the chain, however, due to the complex synthesis and lower molecular weight this is not the first alternative. 2) Reinforce PPS with fillers such as carbon or glass fibres. PPS GF composites are widely used in a range of different industries from food [2] to aerospace [3, 4]. It is known, however that a disadvantage of the introduction of glass fibres into a PPS resin can result in poor interfacial adhesion [5, 6]. A low cost and efficient method to improve the interfacial adhesion is the addition of compatibilizers into the composite but these reduce the thermal and chemical properties of the composite due to the poor thermal and chemical properties of the compatibilizer compared to PPS [6].

The addition of glass or carbon fibres into thermoplastics polymers provides a beneficial increase in mechanical properties. Such fibres are used across a range of other thermoplastics, including nylon [7], poly(ether ether ketone) [8] and poly propylene [9]. Fibres can be introduced into a composite in short (discontinuous) or long (continuous) fibre structure. The manufacturing methods for short and

long fibres are quite different. Short fibre composites are usually mixed within a polymer melt before forming in comparison to long fibres that are generally layered in sheets with a polymer matrix [10]. When short fibres are used as a strengthening mechanism, this typically produces a component equally strong in all principle directions, due to the random orientation of the fibres within the polymer matrix.

Fibre reinforced thermoplastics are susceptible to changing properties as a result of exposure to environmental weathering (UV radiation and moisture) [11]. Long term UV exposure on fibre filled PPS has shown to influence the strength, modulus and glass transition temperature as a result of exposure. A reduction in these thermal and mechanical properties, through photo-oxidation, can compromise the known specification of a component and result in premature failure [12]. The effects of environmental degradation are largely limited to the surface of the component, however over prolonged time in the environment the accumulation of these degrading properties may impact the ability of the component to withstand mechanical loading and crack initiation significantly.

The component analysed within this paper was fabricated using injection moulding and containing short fibres. The injection moulding method applied for this component sees the molten polymer material contained within a heated chamber. A screw-feed mechanism injects the molten polymer material in to a two-part die with a hollow recess which is filled by the molten polymer, in the shape of the component being fabricated. The top die is removed, and an ejector system pushes against the underside of the polymer component to remove it from the lower die. The ejector mechanism as part of an injection moulding process route does inevitably leave flattened sections on the surface of the component. Injection moulding is used primarily due to the lower costs involved within production, and allows the component the structural properties required for typical sports-materials applications.

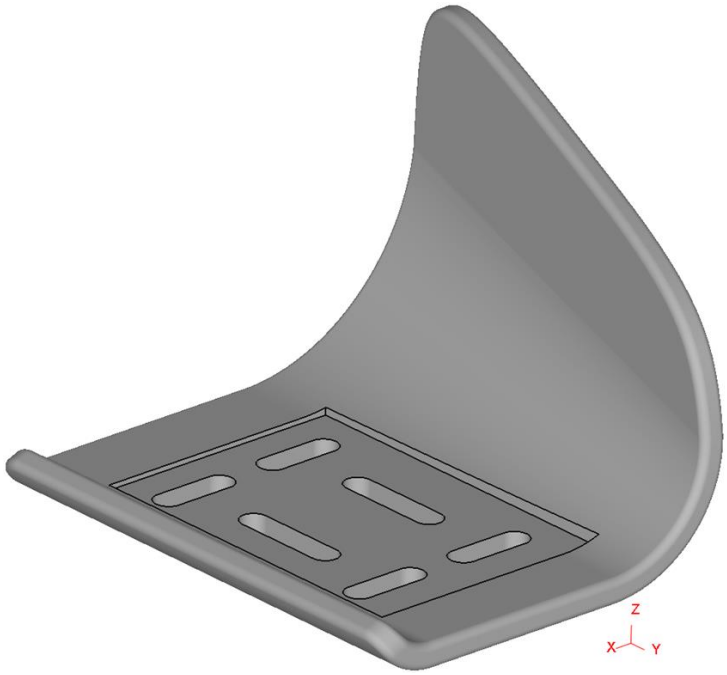

Figure 1: *CAD imaged model of the arm rest component*

Cyclists wish to remain in an aerodynamic position whilst cycling for as long as possible. The posture held by the cyclist is of critical importance to reducing the drag coefficient of the cyclist-bike system [13, 14]. The posture known as the ‘Obree position’, named after cyclist Graham Obree, in which the

cyclists' hands are in support under the chest, the forearms tucked on the biceps, the trunk tilted forward, was found to be the optimal posture for aerodynamic drag reduction [14]. However the position was not considered to be compliant with UCI regulations. A more traditional aerodynamic posture has thus been adopted by professional and club cyclists alike - determined to be the next most aerodynamic by research [14] - whereby the forearms are parallel to the frame of the bicycle, an approximate 90° angle is formed at the elbow and the cyclist leans forward such that his head is directly above his forearms. In order to assist cyclists in achieving this position so called aligning arm rests have been developed. These components (see F**igure 1**) have a curved wing on their outer edge to prevent the forearm from moving laterally outwards and thus increasing the drag coefficient of the cyclist – bicycle system.

The component is mounted to the handlebars of the bicycle using affixing screws fitted through two of the screw holes created in the part, with a supporting aerobar or plate behind. Whilst in-service, the arm-rest components are likely to experience two modes of loading. The first mode, caused by lateral motion of the arms, sees a force applied on the curved surface of the wing, pushing outwards. The second mode, caused by the weight of the cyclist applied vertically downwards through the shoulders, down the arms and on to the edge of the arm rest where the elbow sits, sees a force applied vertically on this back edge of the arm rest component.

2. Material and Methods

A cycling arm-rest component fabricated from the reinforced PPS using injection moulding methods was used for its intended application by a cyclist. The component was brand new, and fitted to the bicycle in its as-received condition. However the component suffered a sudden failure within days of being first attached and used, with a crack propagating through the component and causing the arm-rest to break in two (see **Figure 2**). Due to the component failing so shortly after first being attached to the bicycle, the failure was not considered to be caused in any way by PPS material surface degradation caused by environmental (UV or moisture) exposure.

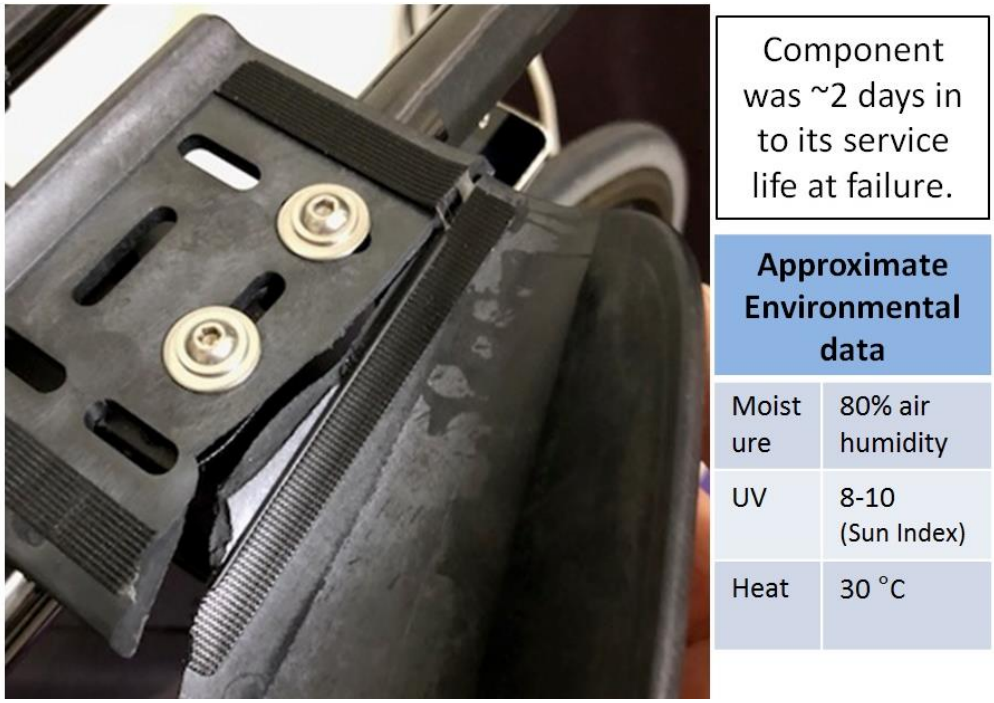

***Figure 2**: Fractured component mounted on the handlebars*

It was of industrial and academic interest to understand why and how the component failed, where the crack initiated from, and whether the component failure was caused by manufacturing-induced defects, abnormal mechanical loading or some other cause. To understand the cause of this sudden fracture of the component better, the material was characterised for its properties, the fracture surface was examined using SEM and Micro CT methods and finally finite element models were constructed to attempt to understand the impact that the in-service loading conditions have upon stress and strain distribution.

2.1 Polymer Measurements

A Perkin Elmer DSC7 was interfaced with a personal computer to measure thermal properties of the composite. The differential scanning calorimeter (DSC) was calibrated using known masses of indium (99.999% pure) and tin (99.999% pure). The composite sample of PPS GF30 (30% glass fibre) was tested using a DSC to determine its thermal properties. A 17 mg sample of PPS was subjected to a heat-cool-heat scan between 50 and 300˚C at 10˚C/min. Crystallisation and melting temperatures were recorded as 282.9 and 244.8˚C respectively. Injection moulding components are cooled rapidly to increase production. This rapid cooling prevents the completion of non-isothermal crystallisation. An exothermic peak at 118.9 ˚C shows this incomplete crystallisation during manufacture (see **Figure** 3). The mechanical properties for the reinforced PPS material were obtained from the literature [15], and can be seen in **Table 1**.

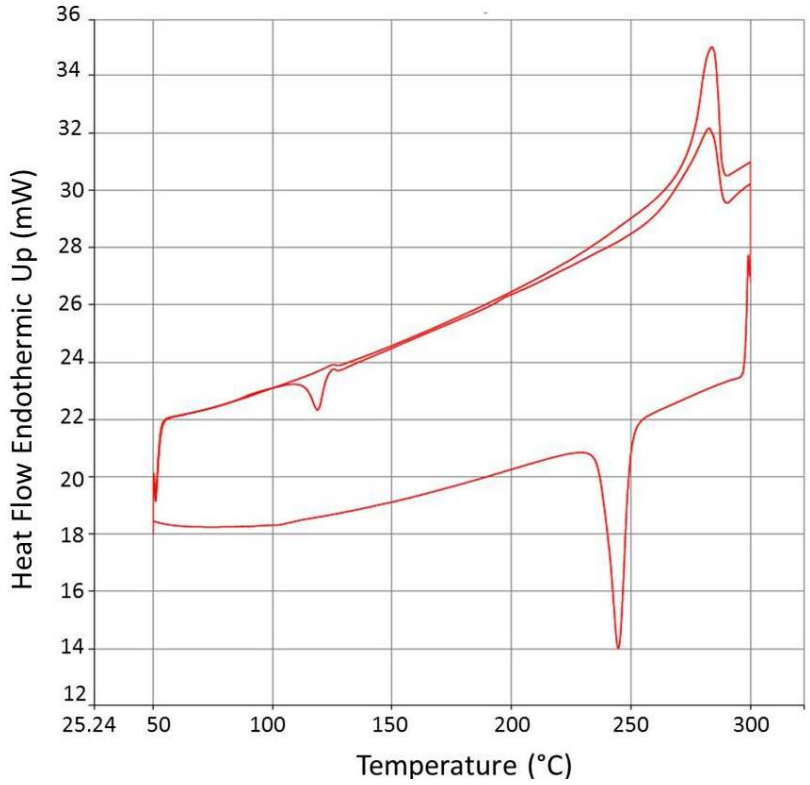

***Figure 3**: DSC trace of PPS GF30*

Table 1 - *Mechanical Properties of PPS GF30 [15]*

Tensile Strength	160 MPa
Tensile Strain at Break	1.75 %

Bending Strength	185 MPa
Bending Modulus	12 GPa
Compression Strength	145 MPa
Young's Modulus	10GPa
Poisson Ratio	0.33

2.2 Failure Analysis

The failed PPS reinforced component required materials characterisation methods to study the fracture surface and the component rigorously. A Hitachi TM3030 scanning electron microscopy (SEM), part of the Centre for Electron Microscopy (CEM) at the University of Birmingham, was used for morphology analysis of the fractured component. The SEM was operated at an accelerating voltage of 15 kV. The SEM analysis for the analysed component is presented in **Figure 4.**

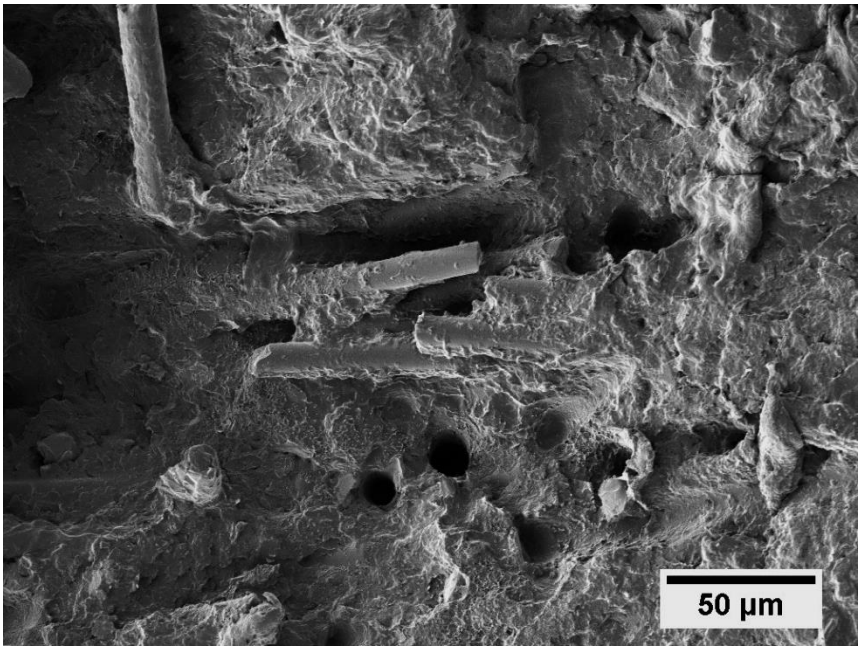

Figure 4: *SEM image at the fracture surface of the component at 500x magnification*

An important aspect of composites created from a polymer and fibre is the adhesion between the fibre and the matrix. Poor adhesion can result in small micro-voids forming, and this may result in stress concentration sites between the two materials. **Figure 4** shows an SEM image of the fracture surface where the fibres show reasonable embedding in the matrix, with no obvious visible voids between the fibres and the matrix. The light grey cylinders represent the glass fibres, of an average length of ~50 µm, within the dark grey PPS polymer matrix. Some evidence of fibre pull-out from the matrix is also observed – these being the two exposed holes in the matrix where fibres used to be embedded.

However, under mechanical loading such as the in-service conditions of this component with the forces applied by the cyclist, the distribution of the loading across the fibres and the matrix needs to be considered, which in turn depends upon fibre orientation [16] The fact that this component is produced with short fibres allows it to be isotropically strong. This would suggest that during normal service loads below the material yield strength, the reinforced polymer would allow for a rebalance of the forces transmitted via the fibres and the matrix in proportion with the strength of the separate phases such that the imparted strain is constant across the two, thus the two phases of the composite remain fully aligned, with no delamination.

Further, a NikonXTH225 Micro CT scanner, again a part of the CEM suite of equipment at the University of Birmingham, was used for tomography analysis with the Micro CT system operating using 110 kV and 110µA. In this configuration, a projection was collected every 1˚ and two frames were obtained for every projection.

3. Theory

3.1 Criteria for sudden fracture

The sudden-onset fracture failure of the PPS arm-support component is hypothesised to have occurred due to one or more of a number of possible criteria. The crack, which has propagated along the sharp corner of the recessed region of the base, must have initiated at a specific location. One hypothesis to explain the catastrophic failure of the part is that a loading on the part, caused by the lateral movement of the cyclists arm, initiated a stress field within the component that allowed a crack to propagate. The likely initiation site within the component to satisfy this hypothesis would be a manufacturing-induced defect, potentially a void or a delamination at the glass fibre particulate / polymer matrix interface.

The second hypothesis to explain why a sudden-onset failure may have occurred suggests that the positioning of the supporting base-plate beneath the arm rest creates a pivot point, about which a vertically applied loading from the cyclists arm pushing down causes a stress-field to be generated within the component. The peak stress experienced by the component in between the screw-holes of the component.

3.2 Finite Element Analysis

A finite element (FE) model was created, using general Finite Element solver Deform v11.1, to better understand the plastic strain and residual stress fields developing within the component, during the loading scenarios that were considered likely based upon the service and the crack surface. The model was constructed from the .step CAD files provided by the manufacturer. The model was set-up in a full three-dimensional environment and computed on a 48Gb RAM, 8-core workstation – although the model was run only on a single core. The model was meshed using the standard tetrahedral meshing application of the DEFORM v11.1 code. The mesh that was used contained a reasonably uniform mesh density - although automatic meshing refinement produced finer elements at sharper radii of the component geometrical features - with approximately 100,000 tetrahedral elements, and with an approximate meshing element length of 1.5mm. The applied mesh can be seen in **Figure 5**.

The model was prepared as a purely mechanical simulation, thus no heat transfer was considered between part and atmosphere, and no heat produced in the component due to mechanical work. The component was specified as a plastically deformable object – thus the FE analysis was simulated in a purely plastic set-up. These were understood to be highly appropriate simplifications based upon the sudden fracture of the component. The reinforced polymer material was represented by a series of flow stress curves and material properties at an ambient temperature of roughly 20 °C. The material properties are given in **Table 1 and Figure 6**. The material was assumed to be of a homogeneous nature for the finite element analysis, as opposed to the PPS matrix and strengthening micro-fibres due to the modelling set-up and the requirements for FE calculations. Thus the material properties assigned to the FE analysis were that of the bulk material – a combination of the matrix and the fibre properties.

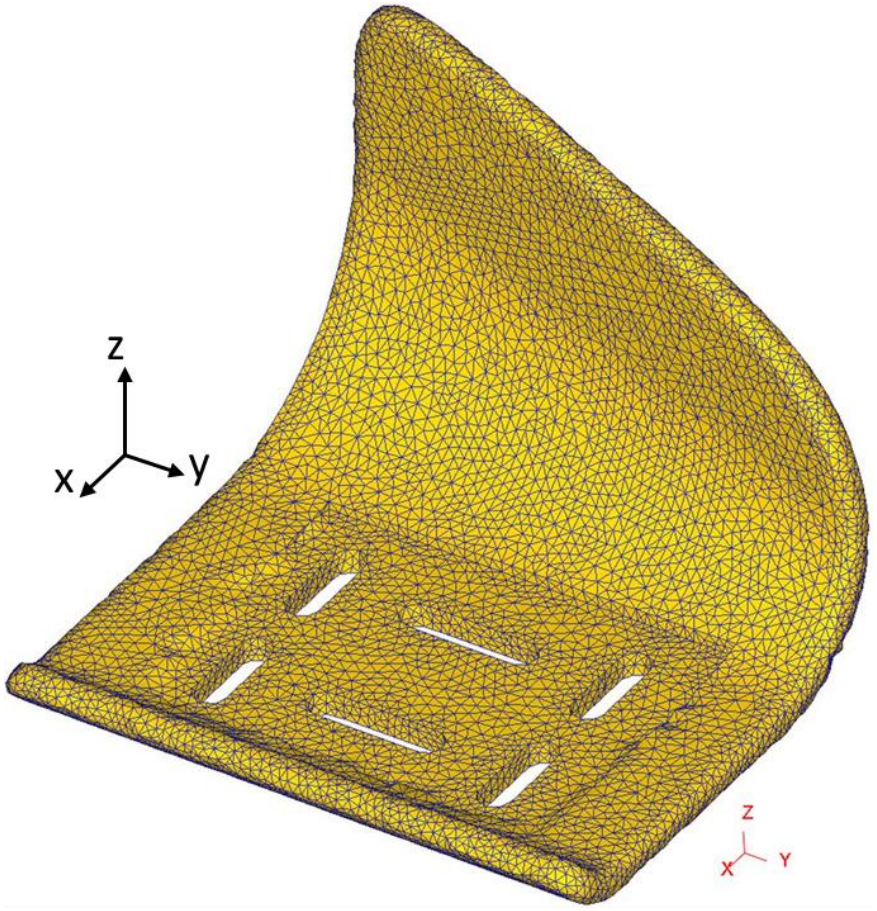

***Figure 5**: The cycling support arm-rest component, imported in to FE software Deform v11.1 and meshed with the automatic meshing tool*

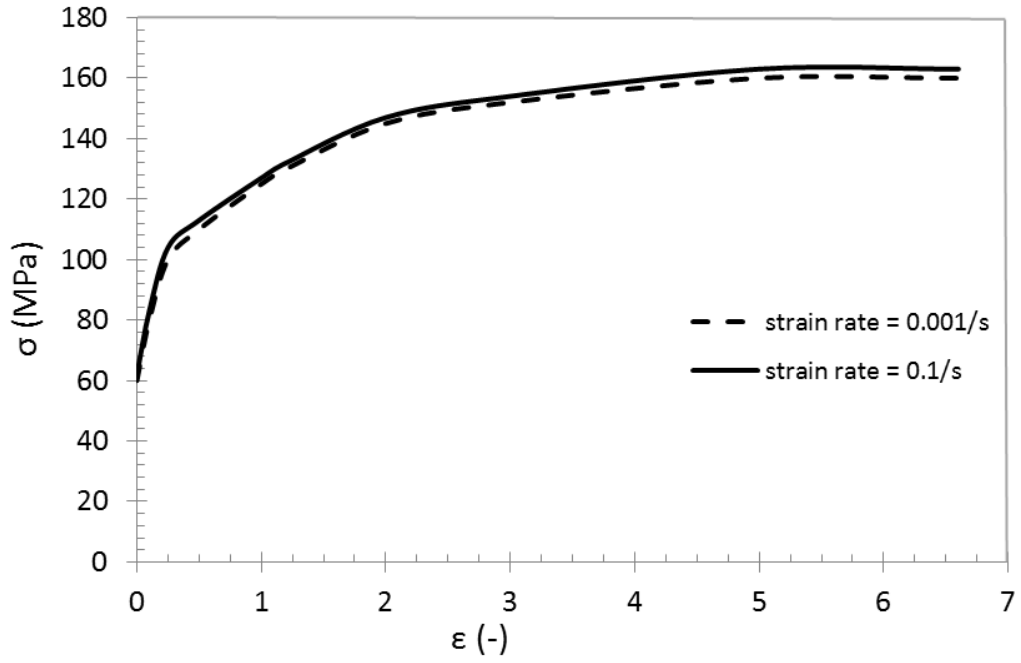

***Figure 6**: Stress-strain graph of PPS GF30 at a strain rate of 0.001 and 0.1/s*

Loading was applied according to the required direction within each individual model. This was applied using a rigid tooling, applying a 1kN force - assumed to be approximately the force caused by the entire mass of the cyclist - for a 'worst-case scenario'. Loadings were applied in the locations as considered in the earlier theory section. A zero-friction condition was applied between the force die and the deformable PPS polymer workpiece. The component was clamped in the vertical axis at the relevant locations where the armrest support was located beneath the armrest.

4. **Results and Discussion**

The FE modelling framework to simulate in-service loadings upon the component for the two loading scenarios considered were performed in FE software Deform v11.1. The outputted predictions for the total strain and the effective (von Mises) stress are presented in **Figure 7.** It can be observed from the predicted strain and stress fields (see **Figure 7a**) that for the lateral loading condition the highest regions of effective (von Mises) stresses and effective strains accumulate along the sharp radius of the recessed flat base section of the component. The von Mises stress values are peaking at approximately 60-70MPa according to FE predictions, which is not of concern given the strength of the material in different loading scenarios ranges from 145-180MPa.

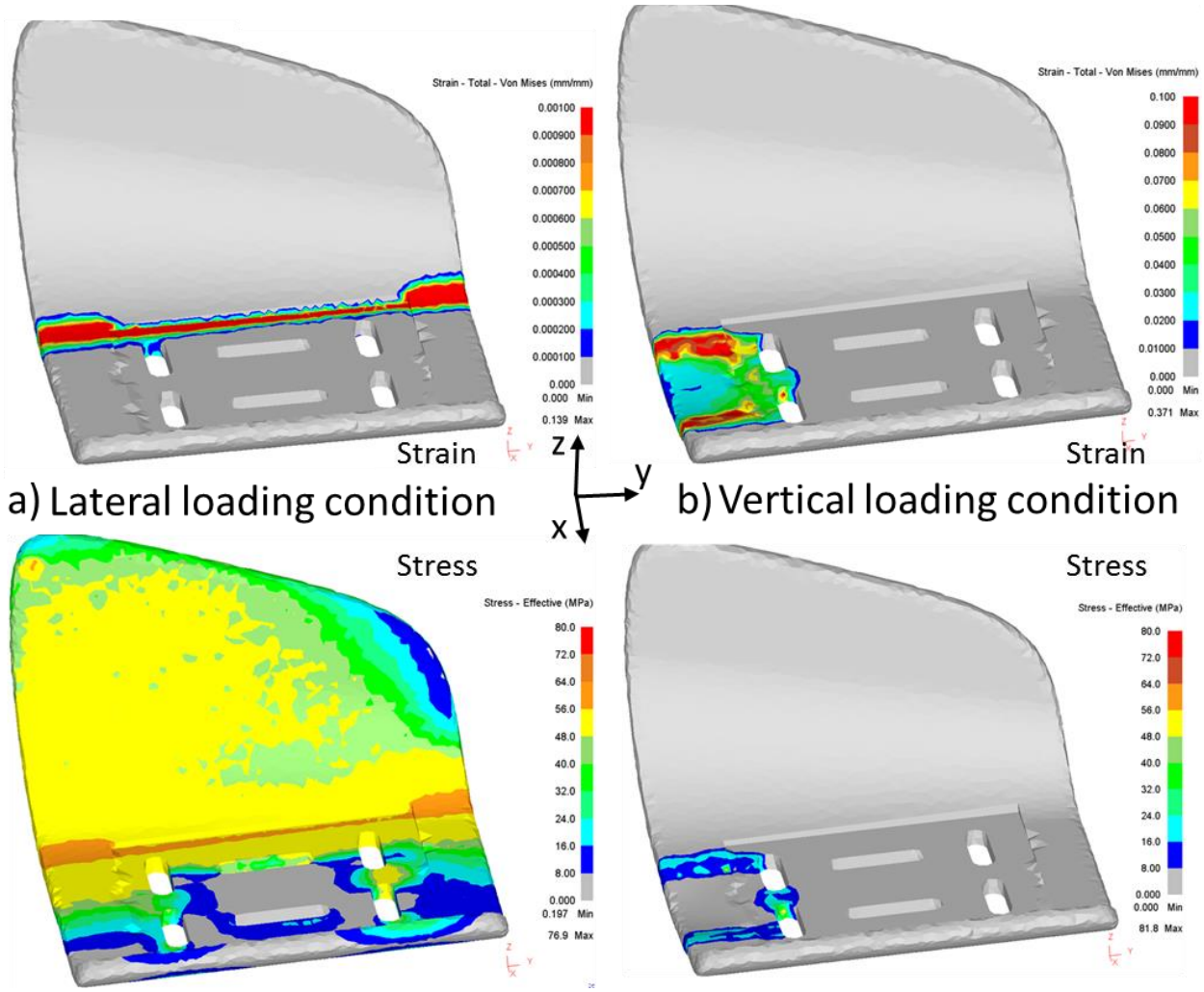

***Figure 7**: FE predictions for plastic strain and Effective stress fields under the two loading conditions*

It is hypothesised that at the moment of failure the component experienced abnormal loading, potentially caused by an uneven road surface which may have induced a mechanical shock in to the system. Mechanical shock is a sudden acceleration caused by impact of an object external to the system [17]. Thus, the forces experienced by the component at the instance of fracture may not simply be produced by the mass of the rider under gravitational acceleration, but now are the summation of this internal system force and the external (mechanical shock) force applied due to the acceleration. The more sudden the shock is, so the acceleration increases and thus so does the force upon the component. It has been demonstrated in the literature that even relatively small impact can produce considerable shock when the time-frame is short [17-18]. The inclusion of mechanical shock will likely have a dual purpose upon the component system, firstly the rider in this situation is highly likely to push out their arms further than usual, exacerbating the lateral loading upon the component. Secondly, the summation of the forces acting upon the component at the critical regions along the sharp corner and in-between the affixing holes will now potentially exceed the loading applied by the rider alone.

However, this will force the component to flex along this corner placing one surface in to tension and the other in to compression, providing a potential driving force for any accumulation of damage and cracking to propagate entirely along the recessed section radius. By comparing to the real component that suffered sudden-onset failure (shown in **Figure 2**), it can be clearly observed that the crack path propagated along much of the sharp-radius corner of the recessed base section where it meets the curved wing. It is therefore highly likely that the driving force to exacerbate the crack propagation came from a lateral force as the cyclist's arm slipped during service.

Whereas, when the component is subjected to the vertical loading condition, a small location of high von Mises stress and strain accumulates in between the two affixing holes within the component closer to the vertical force provided (see Figure 7b) and around the radii of these two affixing holes. The region in-between the affixing holes will likely be subject to crack propagation driving forces associated with regions of high stress, and potentially this just requires an initiation site to provide potential failure. As described previously, characterisation and analysis of the fractured component was carried out using Micro CT. These experiments provide detailed information about the internal structure of the component. The bulk component was observed as a dense solid with no sporadic voids visible confirming complete filling of the mould during manufacture. However, a single void in the component was clearly visible in the Micro CT scan along the surface of the crack (**Figure 8**).

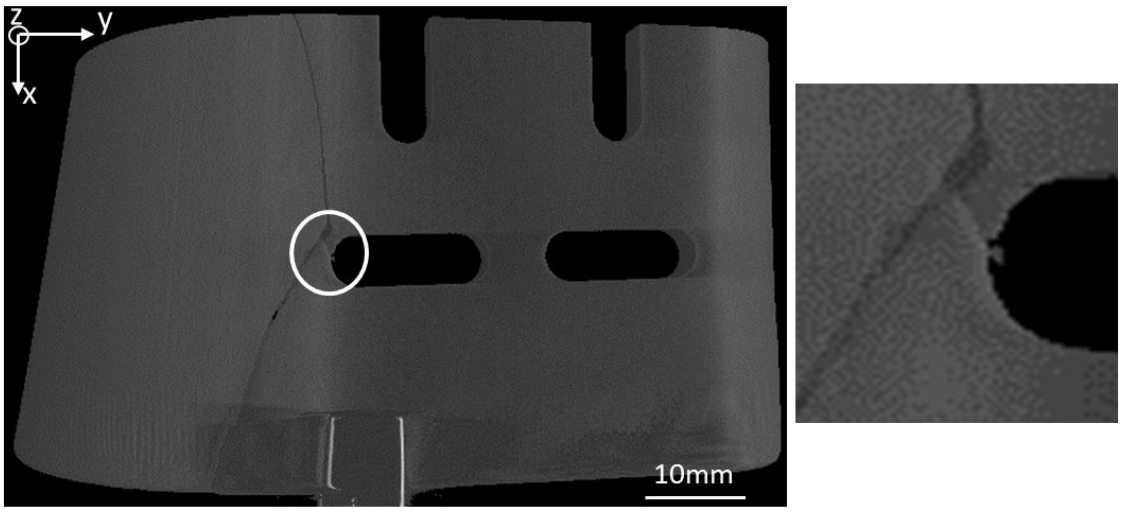

Figure 8*: Micro CT image of a void on the crack interface within the component. An additional crack is indicated as another region of interest (circled) and is zoomed in on the right*

This void, due to the location of the actual crack surface may be a consequence of either; a) the component fracture and a subsequent loss of material in this location due to damage accumulation, or b) an incomplete moulding process leaving a residual void prior to the component failure. The location of the void - well away from any sharp or small features which may restrict the flow - would likely not suggest an incomplete mould operation and thus the observed void probably a result of the loss of material due to high localised damage at the onset of cracking. However, the direction of the crack from the fixing hole to the void would suggest that a weak point may have been present prior to the sudden-onset failure of the component.

Also observed within **Figure 8** is a crack emanating from the left edge of the left affixing hole, and which joins the main crack which propagated through the component. This crack observed with Micro CT methods is noted to match a location of increased stress and strain from the FE predictions for the vertical loading arrangement. Although the highest region of stress and strain was on the other side of the affixing hole, in the region of material between the two, the presence of the through thickness main crack may have changed stress fields in the component, if we assume this is a subsequent crack. Alternatively, this small crack leading from the affixing hole to the main crack may be another potential nucleation site for the sudden failure, although this seems more unlikely.

Finally, the location of the arm rest upon the customer-mounted supporting aerobar was believed to influence the failure of the component in this instance. The location of the supporting bar can be varied to accommodate the riders shape, size and riding preference. Two bolts are used to secure the arm rest. The user can choose from the available six affixing holes manufactured in to the component. The two affixing holes used to support this fractured component are shown in **Figure 9** (represented by the grey circles) from a choice of the six available (represented by the dotted lozenges). The black rectangle represents the support that was situated between the bar and the arm rest. It can be observed that the unused horizontal pair of affixing holes on the left of the image is situated on the very edge of the supporting bar. In this configuration, it is likely that the overhanging region acts as a lever for the loading to be applied and with the fulcrum across the centre of the fixing holes where there is a reduced amount of material.

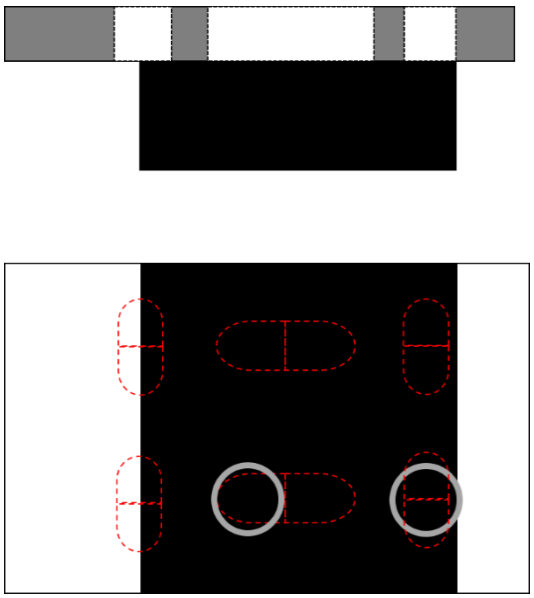

Figure 9: The arm rest location mounted on the aerobar support.

As such, the failure of the component is believed to have occurred as a result of the generation of stress fields within the component that were predominantly formed by a lateral motion of the arm. The fracture along the sharp radius of the recessed base observed within in the actual component strongly supports this theory. However, the additional presence of the vertical loading caused by the mass of the cyclist leaning on to the component, combined with the unfortunate positioning of the supporting aerobar will have likely generated an additional peak in von Mises stress at the location in-between the unused affixing holes. Based upon the reported strength of the material, the levels of stress predicted within the component should not be overly concerning. An additional mechanical shock imparted by an uneven road surface may have increased the loadings applied upon the component at the instant of fracture, increasing the peak values of the stress and strain fields experienced although this is just hypothesis. However, these through-process stress fields, in the presence of any manufacturing route induced defect such as porosity due to an incomplete moulding process, or a delamination of polymer matrix and reinforcing fibres, will act as a stress concentrator effect, and potentially provide an initiator site for a potential sudden fracture of the component. Note that experimentally gathered evidence for crack propagation did also indicate the radii of the unused affixing holes as a potential initiation site.

5. Conclusions

A PPS polymer arm support for cyclists catastrophically failed in-service, leaving the part fractured in to two pieces. The manufacturers were keen to understand whether this was due to unforeseen operating conditions causing overloading of the component, or due to a manufacturing induced defect. The following conclusions are drawn:

- Microscopy analysis of the crack surface has been unable to identify with certainty a nucleation site for the catastrophic failure. However a likely candidate crack initiation site has been identified. Evidence of voids along the crack surface is observed. However, it is uncertain whether these voids were present prior to failure as manufacturing defects in the component, or whether they have formed after failure, as an accumulation of damage at highly strained regions.
- Finite element analysis has been considered for the component under the two obvious loading conditions, with lateral and vertical forces. The lateral force model suggests a localised stress and strain field is concentrated along the curved corner of the component, and at the sharp radius of the recessed base of the component. This is caused by an accumulation of stress along this feature, which potentially acts as a stress concentrator within the component.
- The vertical applied force FE model suggests that for this loading scenario, the peak stresses and strains are experienced in between the screw-holes of the component. This is likely exacerbated by the positioning of the supporting aerobar used in this case. This does match the experimentally observed cracking within this region of the component, although again it is difficult to categorically determine this to be the initiating source of the damage leading to catastrophic failure.

Acknowledgements

The work undertaken within this paper has been conducted as a part of the ERDF part-funded AMCASH programme. AMCASH is a project based at the University of Birmingham and aimed at

supporting regional SME (Small – Medium Enterprise) organisations with academic support in the areas of polymer science, materials characterisation, microscopy and computational modelling. Many thanks are offered by the authors to the ERDF for part-funding the programme.

References

1. Haubs, M. and R. Wagener, Poly(phenylene sulfide) – some news on an old polymerization, in *e-Polymers*. 2002.
2. Yonggang, Y., et al., Synthesis and properties of a copolymer of poly(l,4-phenylene sulfide)–poly(2,4-phenylene sulfide acid) and its nano-apatite reinforced composite. *European Polymer Journal*, 2003. 39(2): p. 411-416.
3. Wayne, H., H.W. Hill, and D.G. Brady, E*ncyclopedia of Polymer Science and Engineering*. Vol. 11. 1988, New York: Wiley.
4. Yu, S., et al., The characteristics of carbon nanotube-reinforced poly(phenylene sulfide) nanocomposites. *Journal of Applied Polymer Scienc*e, 2009. 113(6): p. 3477-3483.
5. Lee, B.S. and B.C. Chun, Effect of nylon66 addition on the mechanical properties and fracture morphology of poly(phenylene sulfide)/glass fiber composites. *Polymer Composites*, 2003. 24(1): p. 192-198.
6. Ren, H.-H., et al., Effect of polyphenylene sulfide containing amino unit on thermal and mechanical properties of polyphenylene sulfide/glass fiber composites. *Journal of Applied Polymer Science*, 2018. 135(6): p. 45804-n/a.
7. Wu, S.-H., et al., Mechanical, thermal and morphological properties of glass fiber and carbon fiber reinforced polyamide-6 and polyamide-6/clay nanocomposites. *Materials Letters*, 2001. 49(6): p. 327-333.
8. Mehmet-Alkan, A.A. and J.N. Hay, The crystallinity of PEEK composites. *Polymer*, 1993. 34(16): p. 3529-3531.
9. Nayak, S.K. and S. Mohanty, Sisal Glass Fiber Reinforced PP Hybrid Composites: Effect of MAPP on the Dynamic Mechanical and Thermal Properties. *Journal of Reinforced Plastics and Composites*, 2010. 29(10): p. 1551-1568.
10. William D. Callister, J. and D.G. Rethwisch, Materials Science and Engineering, *in Materials Science and Engineering, B*. Stenquist, Editor. 2014, John Wiley & Sons Ltd: Asia.
11. A. G. Airale, M. Carello, A. Ferraris, L. Sisca, Moisture effect on mechanical properties of polymeric composite materials, *AIP Conference Proceedings,*2016, 1736:(1) DOI: 10.1063/1.4949595
12. K.B. Mahat, I. Alarifi, A. Alharbi, R. Asmatulu, Effects of UV Light on Mechanical Properties of Carbon Fiber Reinforced PPS Thermoplastic Composites, *Macromol. Symp*. 2016, 365, 157–168. DOI: 10.1002/masy.201650015
13. García-López, J., et al., Reference values and improvement of aerodynamic drag in professional cyclists. *Journal of Sports Sciences*, 2008. 26(3): p. 277-286.
14. Grappe, F., et al., Aerodynamic drag in field cycling with special reference to the Obree's position. *Ergonomics*, 1997. 40(12): p. 1299-1311.
15. Ticona Engineering Polymers - PPS Glass Reinforced, Ticona, Kentucky 41042 USA (2007).
16. R. Blanc, C. Germain, J.P. Da Costa, P. Baylou, M. Cataldi, Fiber orientation measurements in composite materials, *Composites A: Applied Science and Manufacturing*, 37:2 (2006) pp197-206
17. A.J. Brammer, Chapter 10 - Vibration, Mechanical Shock and Impact (*Standard Handbook of Biomedical Engineering and Deisgn*). McGraw Hill (2004).
18. C. Lalanne, Mechanical Shock: *Mechanical Vibration and Shock Analysis - 2nd Edition,* Wiley Online Library (2004). DOI: 10.1002/9780470611913